ACADEMIA ROMÂNĂ
Revue Roumaine de Chimie
http://web.icf.ro/rrch/

Rev. Roum. Chim.,
2014, *59*(9), 769-779

CHARACTERIZATION OF ORGANOMONTMORILLONITE (ORGANO-MMT) AND STUDY OF ITS EFFECTS UPON THE FORMATION OF POLY (METHYL METHACRYLATE)/ORGANO-MMT NANOCOMPOSITES PREPARED BY *IN-SITU* SOLUTION POLYMERISATION

Soufiane BOUDJEMAA[a,*] and Brahim DJELLOULI[b]

[a] Department of Matter Science, Bordj-Bou-Arreridj University, Bordj-Bou-Arreridj, Algeria
[b] Department of Chemical Process Engineering, Sétif University, Sétif, Algeria

Received July 20, 2014

Poly (methyl methacrylate)/montmorillonite nanocomposites were prepared by in situ solution polymerization of methyl methacrylate monomer (MMA) in the presence of the organic modified MMT-clay (OMMT). The results showed that the basal space of the silicate layer increased as determined by XRD, from 13.81 to 20.48 Å. The results of XRD and TEM indicated that the modified clays were dispersed in PMMA to form both exfoliated and intercalated PMMA/MMT nanocomposites. The effect of organic modifiers on the properties of the synthesized nanocomposites was studied. PMMA/OMMT with 5 wt % of Organo-MMT gave the greatest improvement in thermal stability. The rheological properties of the PMMA/OMMT composites were investigated using ARES Rheometer operated in the dynamic mode with parallel plate geometry. The storage and loss moduli were increased with increasing the clay content. The stress-at-break was also relatively improved compared to the virgin polystyrene in the same experimental conditions.

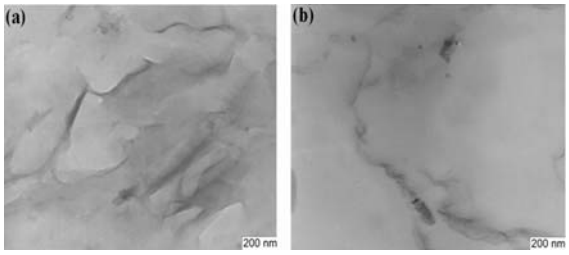

INTRODUCTION

Polymer composites have been widely used in various areas of transportation, construction and electronics products. They offer unusual combinations of stiffness and strength, which are difficult to attain separately from the individual components. On the other hand, polymer layered silicate (PLS) nanocomposites[1,2] are a new class of materials with dimensions typically in the range of 1 to 100 nm. The ultra fine phase dimensions of the nanocomposites leads to their new and improved properties, when compared to their micro- or macro composite counterparts. In recent years, much attention has been paid to polymer-layered silicate nanocomposite, because of its enhanced physical, mechanical strength, thermal stability and chemical properties when compared with those of pure polymer.[3,4] These unique properties of polymer/clay nanocomposites result from high degree of dispersion of clay in polymer matrix. There are two distinct nanostructures identified in these nanocomposites, intercalated and exfoliated.[5] This can be achieved when the nanoscaled silicate platelets are well dispersed by delaminating of the layered silicate throughout the polymer matrices which results the so called exfoliated morphology. The exfoliated nanocomposite

* Corresponding author: bsouf77@yahoo.fr

is more desirable than the intercalated one because of the stronger synergistic effects between polymer matrix and silicate layers.[6] However, it is still a challenging work to obtain the complete exfoliation of clay in polymer.

PMMA (Poly methyl methacrylate) has several desirable properties such as good flexibility, hard and stiff, low water absorption, and outstanding outdoor weathering. However, its poor thermal stability has limited its application. To improve the heat resistance, preparation of nanocomposite is an effective way. PMMA/Clay nanocomposites offer potentials for enhancing tensile strength, and increasing thermal stability. Clays are hydrophilic inorganic compound whereas polymer contains hydrophobic group. Therefore, clays have to be modified by organic modifier containing both hydrophilic and long chain hydrophobic group to increase not only the interlayer spacing, but also the compatibility with polymer matrices. Moreover, clay is naturally occurring, environmentally friendly, cheap and readily available in large quantities. It is evident that polymer/clay nanocomposites can increase strength and stiffness,[1-7] thermal stability,[8] gas barrier property,[9] clarity and decreased flammability[10] with only a small amount of clay.

Recently, radical-initiated MMA polymerization has been applied to prepare PMMA/clay nanocomposites because it is insensitive to water, air, and other impurities. The preparation of PMMA/clay nanocomposites through emulsion,[11] suspension,[12] bulk, and solution[13] polymerization has been reported in the preparation of exfoliated polymer nanocomposites. In this paper, we have prepared the PMMA/clay nanocomposites by free-radical polymerization using benzoyl peroxide (BPO) as initiator. Being hydrophilic by nature, pristine MMT is not suitable as the starting material for the polymer nanocomposites. Therefore, modified montmorillonite is made by quaternary ammonium salt. After the organic modification by ionic exchanging with amine salts, the organoclay becomes hydrophobic and compatible with methyl methacrylate monomer. We have discussed herein the effect of modifying agent with different structure on the morphology and properties of the PMMA/clay nanocomposites. The morphology of these nanocomposites has been characterized by wide angle X-ray diffraction (XRD) and transmission electron microscopy (TEM). The thermal and gas barrier properties of these nanocomposites have been studied by thermal gravimetric analysis (TGA) and differential scanning calorimetry (DSC). The rheological properties of polymer/clay nanocomposites are determined by a combination of microscopic structure and the strength of the interaction between the polymer and clay. Due to this kind of internal structure, polymer/clay nanocomposites have provided important characteristics of the static and dynamic properties of confined polymer including viscoelastic properties.[14,15]

In the present work, Algerian montmorillonite was organophilized and tested to prepare nanocomposite by In-Situ Solution Polymerisation. The results in terms of thermal, rheological, and mechanical properties of nanocomposite are presented as a function of clay contents.

MATERIALS AND METHODS

1. Materials

Ruffian montmorillonite with cationic exchange capacity of 95 meq/100g was supplied by the County of Maghnia, Algeria, and used after purification. Methyl methacrylate (Aldrich, 99%), Benzoyl peroxyde (Alfa Aesar, 90%), n-hexane (Technical, 99%), Toluene (Biochem.chemopharma, 99.8%) were used as received without further purification. The modification agent is n-hexadecyltrimethyl-ammonium chloride HTACl (Alfa Aesar, 96%).

2. Sodium montmorillonite (MMT-Na) preparation

The original clay mineral used in the present work was Maghnia montmorillonite. It was isolated from Maghnia clay (Algeria) by successive decantation from the aqueous suspensions. The raw material was dried in the oven at 110°C for four days, ground in an agate mortar and sieved in 100 μm filter. The obtained powder was immersed in a H_2O_2 (30%) solution for 48 h in order to eliminate the organic materials. The clay suspension was then washed seven times in distilled water at 30°C using the centrifugation process. Dried at 50°C for five days, the precipitate was sieved in 100 μm filter. 170 g of the prepared clay was dispersed in 5 L of (1 M) NaCl solution and stirred for 30 min at 40°C using the centrifugation method. The procedure was repeated four times and the obtained suspension was kept for 48 h. The precipitate was collected by filtration and rinsed with distilled water at 80°C until an $AgNO_3$ test verified the absence of chloride. Dried at 80°C for 48 h, ground in a mortar and sieved

with 100 μm filter, the MMT-Na was stored in a vacuum desiccator for five days.

3. Modification of MMT-Na

The organic clay was prepared by cation exchange reaction between the sodium cation of the MMT and modifying agent (HTACl). Typically, 100g of MMT-Na was suspended into 600 ml distilled water and stirred for 1h at 75°C. Then clay suspensions were dropwise slowly added into the modifying agent (34,4g HTACl + 200ml distilled at 75°C). The mixture was stirred vigorously for 2 h at 75°C. The organic modified clay was separated by centrifugation (4000rpm, 7min) then the precipitate was collected on a filter paper, washed three times with distilled water at 65°C under the control of $AgNO_3$. The precipitate was dried to obtain a modified montmorillonite with HTACl (MMT- HTACl).

4. Preparation of the PMMA/ MMT-HTACl Nancomposite by insitu polymerization

The Preparation of PMMA/clay nanocomposites with 1,3 and 5 wt% clay loading, an appropriate amount modified clay (0.1 g) was suspended in 30 ml of toluene under magnetic stirring overnight at room temperature, 9.9g of methylmethacrylate monomer and 0.1g of benzoyl peroxide initiator were added to this solution. Under magnetic stirring, the solution was stirred for 5h at 85°C in a nitrogen atmosphere and the final product was precipitated in 800 ml of n-hexane. The product was dissolved in 30 ml of toluene and re-precipitation process was repeated to obtain more pure nanocomposites. The PMMA/Clay nanocomposites were dried at 45°C in a vacuum for 48h.

5. Characterization

X-Ray diffraction (XRD) patterns were obtained with a Philips diffarctometre (PW-1710) using CuKα (λ=1.54Å) radiation at room temperature. All scanning are performed in 2θ range 2-30 degrees. The basal spacing distance of silicate layers were calculated from the estimation of (001) plane peak in XRD patterns using the Bragg's law:

$$d_{001} = \lambda/2\mathrm{Sin}\theta \qquad (1)$$

The morphology of the clay in the hybrids was observed on a transmission electron microscope (TEM) (JEM2000EXII, 200 kV). The samples with a thickness of 70 nm were prepared by using leica Utracut-UCT. the class transition temperature (T) was determined by using a Shimadzu DSC-60 differential scanning calorimeter (DSC) with N_2 as a purge gas, with a heating rate of 10 °C/min. The thermal decomposition determined by thermal gravimetric analysis (TGA) was conducted on a Shimadzu TGA-51H analyzer with N_2 as a purge gas; with a heating rate of 10 °C/min.

The infrared analysis was conducted on a Shimadzu FTIR-8300 spectrophotometer, using KBr disc method. The melt rheological properties of the material were determined using an ARES-rheometer (Rheometrics Scientific, USA). In This work the measurements were performed in the dynamic mode and 8 mm parallel plate's geometry with gap settings about 2 mm under nitrogen gas. The strain amplitude was kept in the linear viscoelastic region in the whole frequency range. The measuring temperature was at 200°C as a function of the angular frequency, ω (rad/s). The frequency is varied between 100 and 0.1 rad/s.

To measure the stress-at-break, six specimens were cut and their thickness was taken at three different places on the specimen. The average for stress-at-break calculation sample was carefully mounted straight and symmetrically in the grips of the dynamometer tester and then was stressed at a constant strain rate until failure. The stress was assessed by the following equation:

$$S = F/A \quad (\mathrm{MPa}) \qquad (2)$$

where: S = stress-at-break; F = applied force; A= cross sectional area.

RESULTS AND DISCUSSION

1. Characterization of modified MMT

The X-ray spectra for powder MMT-Na, and organically modified clay MMT-HTACl are shown in Fig. 1. Bragg's equation, $2d \sin\theta = n\lambda$, was used to calculate the basal spacing of the modified clay MMT-HTACl as well as the pristine clay MMT-Na. The characteristic d_{001} diffraction peak for MMT-Na in the 2θ region is located at 6.39°, d_{001} = 13.81Å. The modification of the clay MMT-Na with HTACl shifts the d_{001} peak to lower values in the 2θ region which are located at 4.31°, d_{001} =20.48 Å for MMT-HTACl. This shift suggests an increase in the basal spacing of the

silicate platelets. The increase of the basal spacing is due to the penetration and grafting of the quaternary salt via ion exchange to the clay platelets. The indexing of the d_{001} peak in the diffractograms of modified clays also suggests that the morphology of the clays is intercalated.[16]

The TGA curves MMT-Na and MMT-HTACl are shown in Fig. 2. MMT-Na displays two thermal degradation transitions. The first one occurs in the temperature range 100–350 °C and is due to the volatilization of both the free water (*i.e.*, the water sorbed on the external surfaces of crystals) and the water residing inside the interlayer space, forming hydration spheres around the exchangeable cation.[17] The second transition takes place at higher temperatures (between 500 and 800 °C) and is owing to the structural water resulting from the dehydroxylation of clay OH units. On the other hand, organically modified MMT follows a four-step decomposition process. The vaporization of free water takes place at temperatures below 200 °C, while the surfactant's decomposition happens in the temperature between 200–500 °C. Dehydroxylation of the aluminosilicates occurs between 500 and 800 °C.[18]

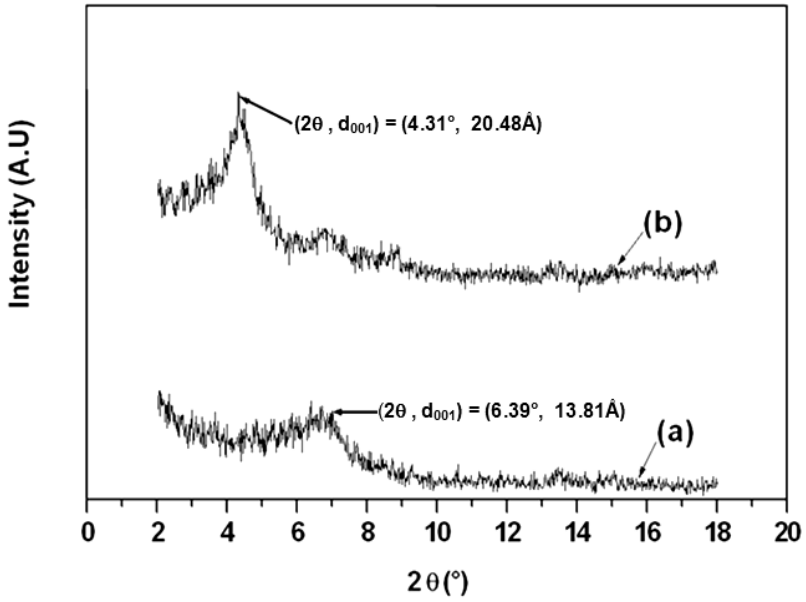

Fig. 1 – XRD pattern of (a) MMT-Na and (b) MMT- HTACl.

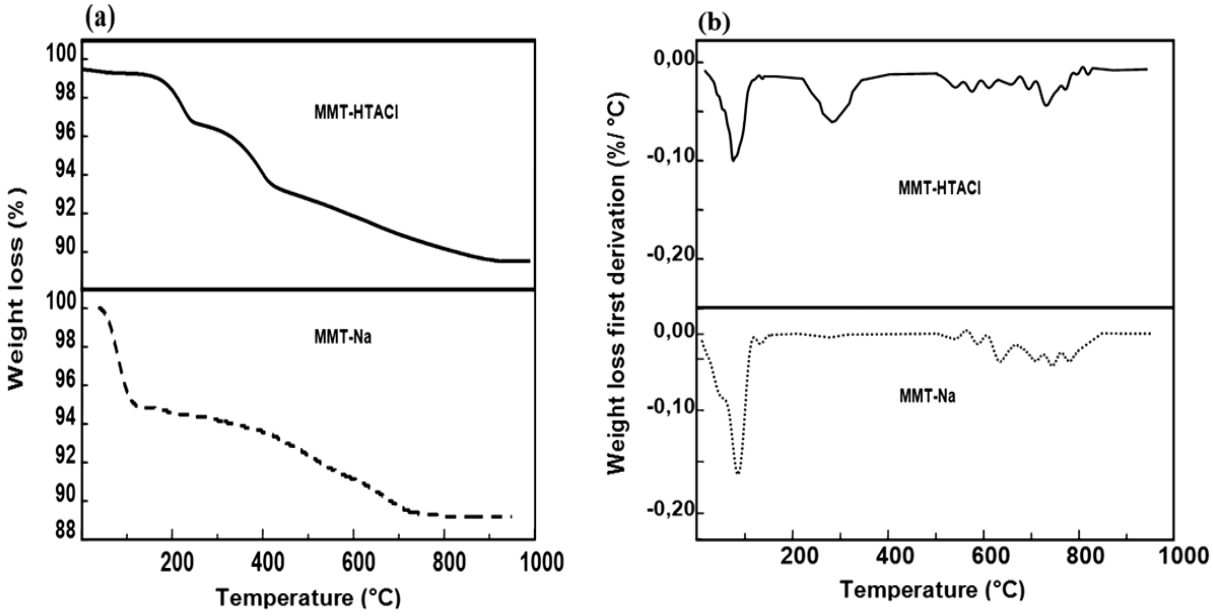

Fig. 2 – **TGA** (**a**) and DTGA (**b**) curves of: MMT-Na and MMT-HTACl.

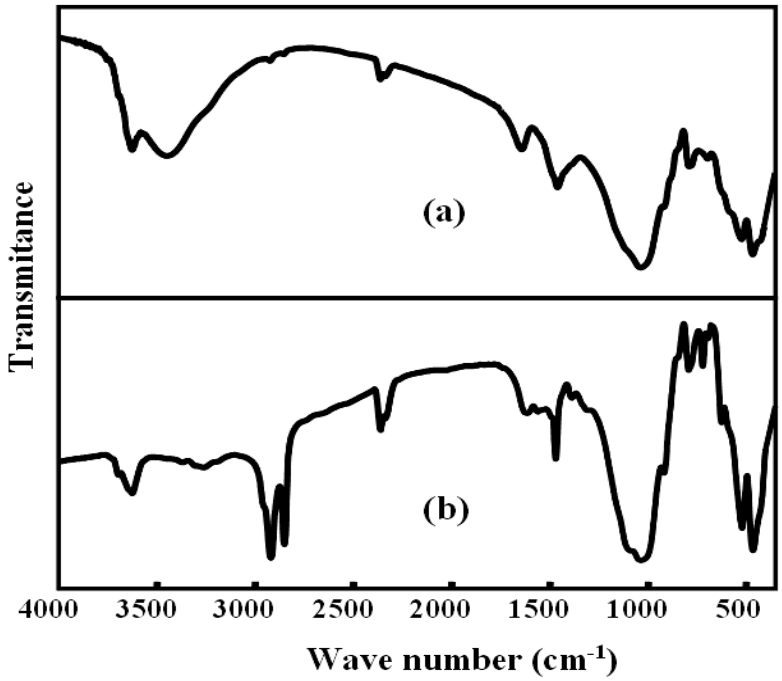

Fig. 3 – FTIR spectra of: a) MMT-Na and b) MMT-HTACl.

FTIR spectra of sodium montmorillonite and those organically modified clays are shown in Fig. 3. As noted, all the spectra show bands at 3636 and 3395 cm^{-1} attributed to O–H stretching for the silicate and water, respectively, 1639 cm^{-1} (related to O–H bending), 1040 cm^{-1} (owing of stretching vibration of Si–O–Si from silicate), 917 cm^{-1} (from Al–OH–Al deformation of aluminates), and 524 and 472 cm^{-1} (Al-O stretching and Si-O bending vibrations of MMT, respectively).[19] However, there are some bands in organoclays samples spectra which are not exhibited by the sodium clay; these bands were located at 2924, 2842 and 1475 cm^{-1} and were assigned to C–H vibrations of methylene groups (asymmetric stretching, symmetric stretching and bending, respectively) from chemical structure of the surfactant.[20]

2. Morphology of the PMMA/Clay Nanocomposites

The structure and properties of layered silicate composites are usually studied by XRD, TEM and dynamic mechanical analysis (DMTA) techniques. Based on the disappearance or the decrease of intensity of XRD peaks, authors conclude the silicate is partially or completely exfoliated.[12] The XRD patterns of PMMA/MMT-HTACl nanocomposites with 1, 3 and 5 wt% modified clay are measured and shown in Fig. 4. Can be seen Fig. 4 b, the peak related to clay is disappeared, suggesting that the MMT silicate sheets are exfoliated in PMMA/MMT-HTACl composites. This assumption is greatly supported by the larger gallery distance of the organophilized filler obtained during the cationic exchange process. The TEM image shown in Fig.5 indicates micro-sized structure where can be seen the primary particles composed of many silicate layers. To further investigate the clay dispersion in the polymer matrix, TEM analysis was performed, as shown in Fig. 5. TEM (Fig. 5 a) indicates micro-sized structure where can be seen the primary particles composed of many silicate layers. This situation corresponds to that of conventional filled polymer where, at least, the primary particles of few microns are dispersed in the polymer matrix. When the amount of organoclay increased to 3% and 5%, there was a small clay peak observed at $2\theta = 2.42°$ (Fig. 4 c, d). This implied that there is a small amount organoclay that cannot be exfoliated in the PMMA which may form intercalated nanostructure.[21] In the corresponding TEM micrograph (Fig. 5 b) is visible a tactoids, indicating a co-existence of micro-sized and intercalated structures.

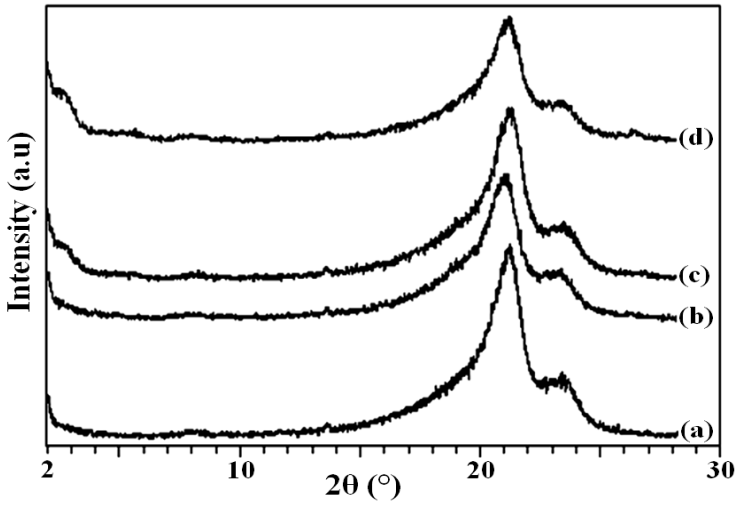

Fig. 4 – XRD Patterns of PMMA/MMT-HTACl composites with different MMT-HTACl contents: (a) 0, (b) 1, (c) and (d) 5 wt%.

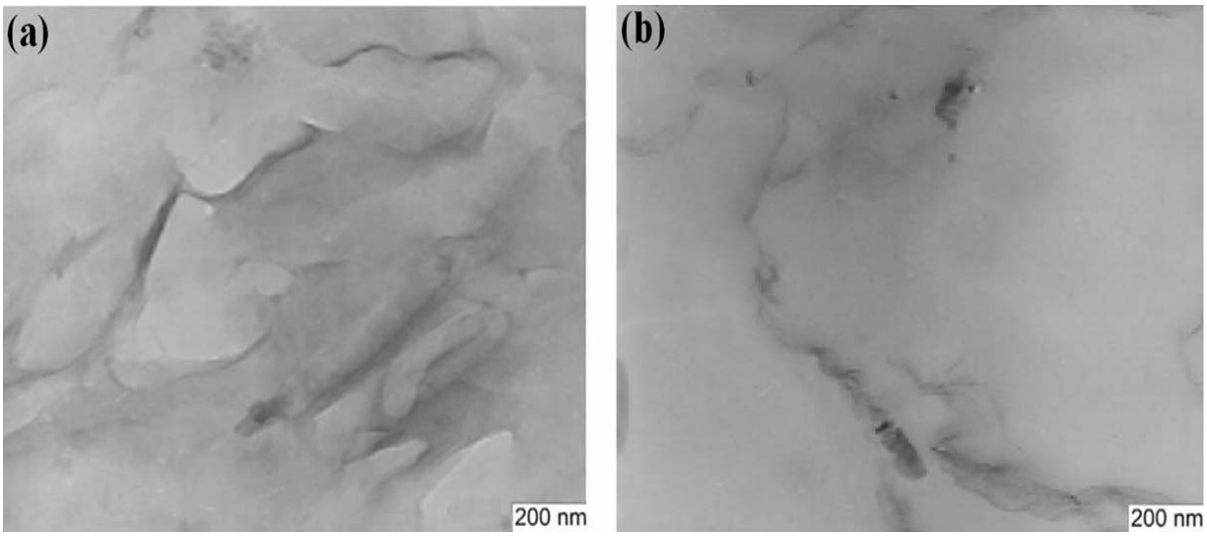

Fig. 5 – TEM image of: (a) PMMA/MMT-HTACl 1 % and (b) PMMA/MMT-HTACl 5%.

3. Thermal Properties of PMMA/Clay Nanocomposites

Fig. 6 reveals higher stability of PMMA/MMT-HTACl composites than pure PMMA. Since the onset of decomposition for PMMA/MMT-HTACl composites is shifted toward a higher temperature with the clay content. For instance, at 10% of degradation, the thermal decomposition temperature $T_{0.1}$ was increased from 388°C for the neat PMMA to 397 °C for the composites containing 1 wt% HTACl (Table 1). However, the composite containing 5 wt% of HTACl shows the highest degradation temperature (418°C). This behaviour is largely maintained throughout the organic decomposition (as shown by the comparable improvement in $T_{0.5}$, the temperature at which 50% degradation occurs) (Fig. 7)[12]. Thus, MMT possesses high thermal stability and its layer structure exhibits great barrier effect to stop the evaporation of the small molecules generated in the thermal decomposition process and effectively limits the continuous decomposition of the PMMA.[13, 14]

Similar observation is deduced from the first TGA derivative of PMMA composites illustrated in Fig. 8, where the peak indicates the temperature at a maximum rate of degradation, delayed at a higher temperature (Table 1). The insertion of PMMA inside the interlayers can be ascribed to both the ion-induced dipole force between clay layers and PMMA, and the contraction of the gallery height due to water removal. Dietsche and Mulhaupt[15] also observed an improved thermal stability of acrylic composites using TGA technique. The relatively strong fixation between polymer and inorganic surface is also considered to be due to the cooperative formation of ion induced dipole forces.[16]

In addition, Chen *et al.*[17] suggested that the higher decomposition onset temperature of a polymer/Organoclay composite as compared to that of polymer can be attributed to the nanoscale MMT layers, preventing out-diffusion of the volatile decomposition products. This may be the reason why the Polymer/Organoclay composite exhibited higher thermal stability than virgin Polymer.

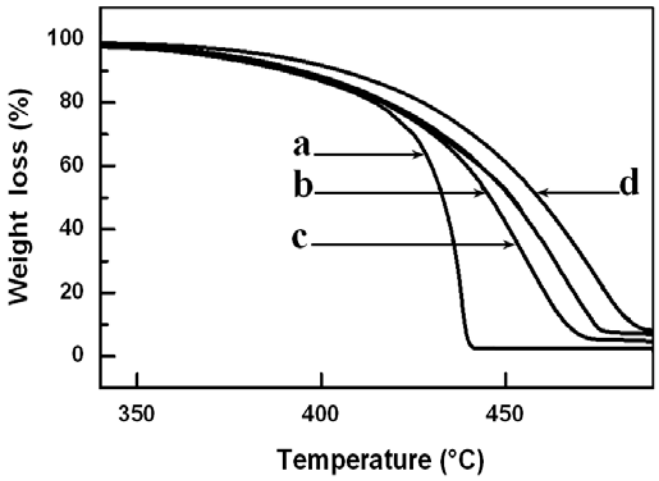

Fig. 6 – TGA Thermograms of weight loss versus temperature of PMMA/MMT-HTACl composites: (a) 0, (b) 1, (c) 3 and (d) 5 wt%.

Table 1

Degradation and glass transition temperatures of PMMA/MMT-HTACl composites with various MMT-HTACl contents (wt %) prepared by solution polymerization

Sample	Tg (°C)	Temperature at maximum rate of degradation (°C) measured by (TGA)	Temperature at % Weight Loss (°C)	
			10%	50%
PMMA- 0% MMT-HTACl	95	440	388	430
PMMA- 1% MMT-HTACl PMMA- 3%	100	458	397	443
MMT-HTACl PMMA- 5% MMT-HTACl	115	470	409	457
	118	481	418	469

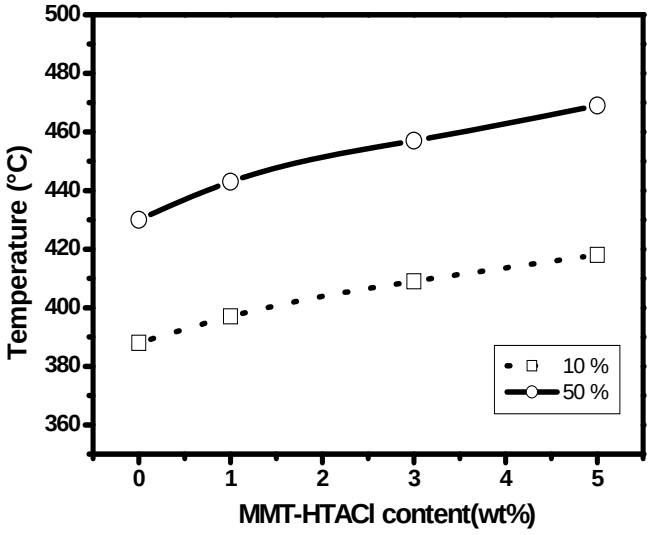

Fig. 7 – Decomposition temperature of PMMA/MMT-HTACl composites.

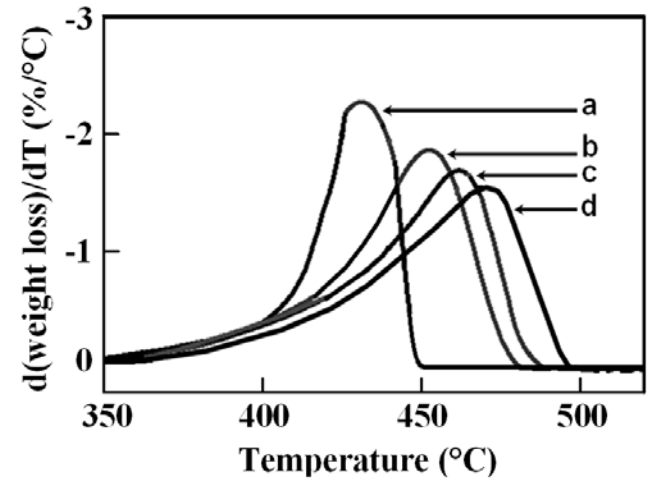

Fig. 8 – TGA derivative of PMMA/MMT-HTAC composites with different MMT-HTACl contents: (a), 0, (b) 1, (c) 3 and (d) 5 wt%.

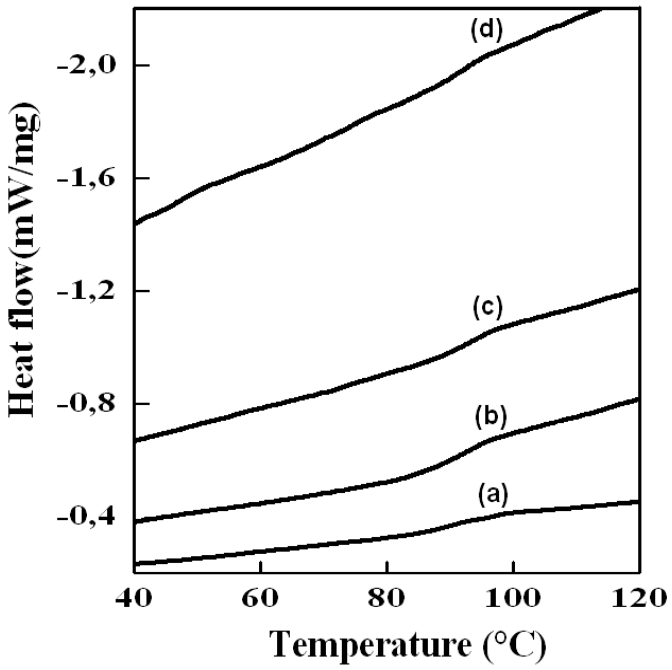

Fig. 9 – DSC thermograms of PMMA/MMT-HTACl composites with various MMT-HTAC content (a) 0 wt%, (b) 1 wt% , (c) 3 wt% , and (d) 5wt%.

To investigate the mobility of PMMA chains in term of its Tg (glace transition temperature) in the clay layers, DSC study of pure PMMA and PMMA/MMT-HTACl hybrids has been carried out (Fig. 9). The glass transition temperature was determined at the inflection point between the onset and the end set temperatures. The Tg of the composites was remarkably increased relatively to the neat poly methyl methacrylate, but slightly as the MMT-HTACl content increases. This is clearly caused by the strong interaction between MMT-HTACl and PMMA, which limits the cooperative motions of the PS main chain segments.[18] The different values are summarized in Table 1.

4. Mechanical and Rheological Properties of PMMA/Clay Nanocomposites

Linear viscoelastic responses, such as storage modulus (**G′**) and loss modulus (**G″**), of unfilled (neat) and filled PMMA are logarithmically plotted

at 200°C as a function of angular frequency in Figs. 10 and 11, respectively. As the silicate loading increased, both **G′** and **G″** show monotonic increase along the entire frequency range. These figures show that the dynamic mechanical moduli of the PMMA composites are higher than those of neat PMMA, in particular at low frequencies, the difference is significant. However, the difference in the dynamic moduli values between PMMA/5 wt% MMT-HTACl and PMMA/3 wt% MMT-HTACl is minimum. The **G′** has slopes of 0.95 (PMMA), 0.89 (PMMA/1 wt% MMT-HTACl), 0.78 (PMMA/3 wt% MMT-HTACl), and 0.75 (PMMA/5 wt% MMT-HTACl) while **G″** has slopes of 0.52 (PMMA), 0.55 (PMMA/1 wt% MMT-HTACl), 0.49 (PMMA/3 wt% MMT-HTACl), and 0.47 (PMMA/5 wt% MMT-HTACl) in log plots indicating that at the lowest frequencies, the response of the system exhibits liquid-like behaviour (**G″** > **G′**). However, the two moduli soon become equal and display nearly a plateau region, having higher **G′** than **G″**.

In this region, PMMA/MMT-HTACl show glassy solid-like behaviour.[19] This characteristic transition (from liquid-like to solid like behaviour) shifts to the low frequency region as the OMMT loading increases. Similar trends in the oscillatory shear experiment were also observed by Krishnamoorti and Giannellis[20] for a series of nylon6/MMT and poly (e-caprolactone)/MMT composites for the polymer chains being end tethered to the silicate surface via a cationic surfactant. The slope and absolute values of the dynamic moduli indicate a super molecular structure formation in the composite.[21] The higher was the ***G′*** and the smaller was the slope, the more pronounced was the interaction between the silicate sheets and their tendency to form a 3-dimentional superstructure.[22] The higher was the ***G′*** and the smaller was the slope, the more pronounced was the interaction between the silicate sheets and their tendency to form a 3-dimentional superstructure.[23] Rheological measurements performed on PMMA-based model composites have shown that the formation of a superstructure results in a well-pronounced equilibrium plateau modulus.[23]

The ratio of ***G″/ G′*** is tan δ and it is plotted semi-logarithmically as a function of frequency for PS and PS composites at 200°C in Fig. 12. This figure indicates that tan δ of PS composites is shown to be nearly independent on the frequency particularly at low frequency range. That independency, is due to the development of the material elasticity. This effect is clearly seen at very low frequency, where a visible difference between tan δ values of neat PS and PS composites is observed. Since, the value of tan δ decreases with increasing the clay content.[22]

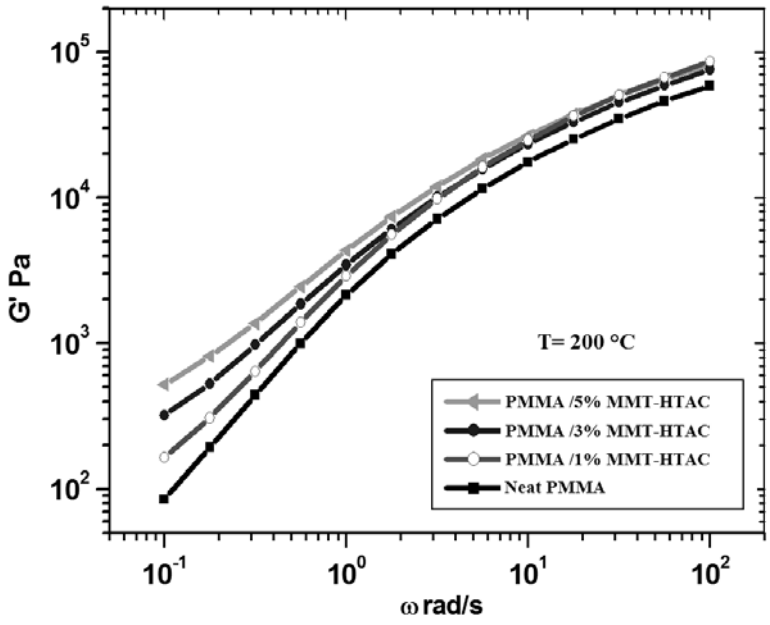

Fig. 10 – **G'** of PMMA and PMMA composites as a function of angular frequency at T= 200°C.

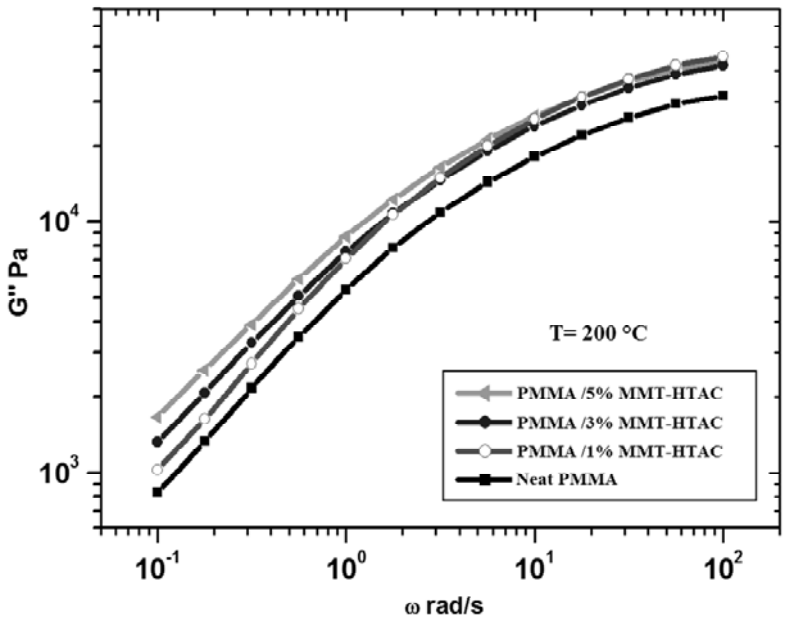

Fig. 11 – **G"** of PMMA and PMMA composites as a function of angular frequency at T= 200°C.

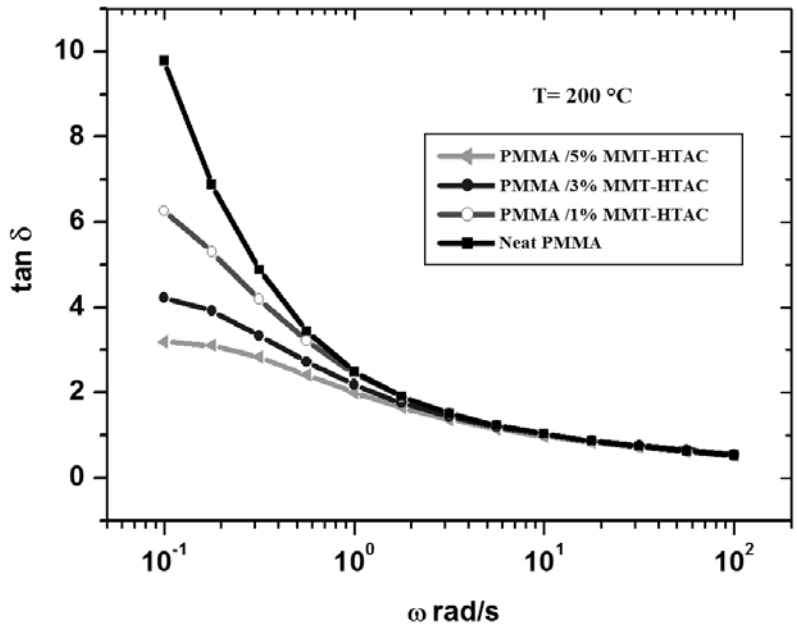

Fig. 12 – tan δ of PMMA and PMMA composites as a function of ω at T = 200°C.

In thermoplastic based (intercalated or exfoliated) composites, the stress-at-break, which expresses the ultimate strength, may vary strongly depending on the nature of the interactions between the matrix and the filler.[24] The stress-at-break of PMMA / MMT-HTACl composites versus organophylic montmorillonite content curve is displayed in Fig. 11. As expected, the silicate reinforced systems show a superior strength relatively to ordinary PMMA. It is obvious that even with the addition of such a low loading of montmorillonite (1-5 wt %), the stress-at-break increases considerably. For instance, compared to unfilled PMMA, the 5 wt% clay composite has around 16% higher tensile strength. On the other hand, the increase of the stress-at-break is more pronounced between 0 and 5 wt% OMMT content. This observation can be attributed to the strong interaction between PMMA and MMT-HTACl.

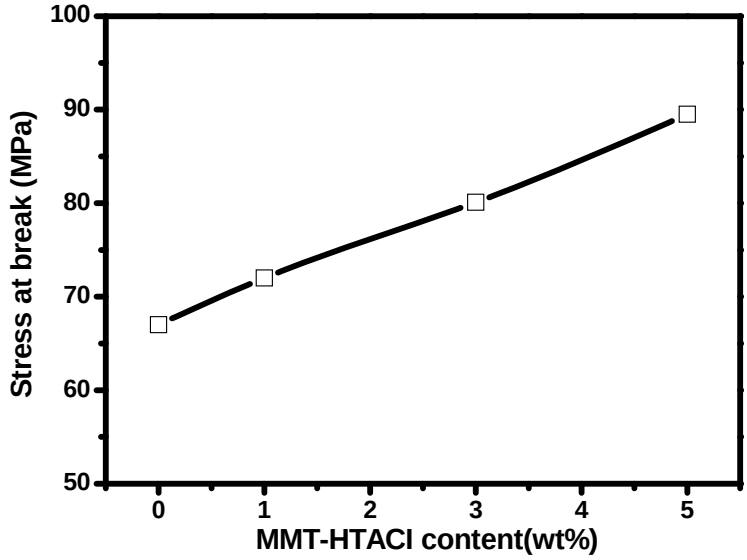

Fig. 13 – Stress-at-break of PMMA/MMT-HTAC composites versusMMT-HTAC content (wt %).

CONCLUSIONS

PMMA/MMT nanocomposites were synthesized by in situ solution polymerization. Algerian montmorillonite was ionically exchanged by trimethyhexadecyl ammonium chloride (HTACl). PMMA/MMT nanocomposites were characterized using different techniques.

The results showed that the basal space of the silicate layer increased. From XRD and TEM micrographs, the Poly (methyl metacrylate) was exfoliated into the silicate layers, and had fine dispersion in the Poly (methyl metacrylate) matrix. Besides, the PMMA/MMT nanocomposites are found to have better thermal stability and mechanical properties than pure Poly (methyl metacrylate) material and depended on clay loading. The optimum organo-montmorillonite content to give the best improvement is 5.0 wt% for thermal stability of nanocomposite. The rheological and mechanical properties were improved by the incorporation of clay into PS. Since the stress-at-break was improved relatively to the virgin polystyrene. The rheological results for virgin PMAA and its derived nanocomposites showed that the dynamic mechanical moduli (G', G" and tanδ) were found to be increased with the incorporation of MMT-HTAC into PMAA and their values tend to increase as the PMMA/MMT-HTAC loadings increase.

Acknowledgments: The authors would like to thank the Department of Matter Science, Universiti Bordj-Bou-Arrerid, and Department of Chemistry, University of M'sila for the provision of laboratory facilities.

REFERENCES

1. E. P. Giannelis, *Adv. Mater.*, **1996**, *8*, 29-35.
2. A. Agag and T. Takeichi, *Polymer*, **2000**, *41*, 7083-7090.
3. H. J. Park and C. S. Jana, *Polymer*, **2003**, *44*, 2091-2099.
4. B. M. Novak, *Adv. Mater.*, **1993**, *5*, 422-431.
5. A. B. Morgan, J. W. Gilman and R. H. Harris, *Polym. Sci. Eng.*, **2000**, *83*, 53-60.
6. T. H. Chen, J. J. Zhu and B. H. Li, *Macromolecules*, **2005**, *38*, 4030-4041.
7. T. LAN, P. D. Kaviratna and T. J. Pinnavaia, *Chem Mater.*, **2000**, *8*, 2150-2159.
8. J.W. Gilman, *Appl. Clay. Sci.*, **1999**, *15*, 49-58.
9. H. Shi, T. Lan and T. J. Pinnavaia, *Chem. Mater.*, **1996**, *8*, 1584-1587.
10. A. B. Morgan, *Polym. Adv. Technol.*, **2006**, *17*, 2006-2013.
11. Y. Li, B. Zhao and S. Xie, *Polym. Interna.*, **2003**, *52*, 898-908.
12. X. Liu and Q. Wu, *Polymer*, **2001**, *42*, 10013-10019.
13. S. D. Burnside and E. P. Giannelis, *Chem. Mater.*, **1995**, *7*, 1597-1600.
14. K. Yano, A. Usuki and T. Kurauchi, *J. Polym. Sci. Pol. Chem.*, **1993**, *31*, 2493-2498.
15. F. Dietsche and R. Mülhaupt, *Polym. Bull.*, **1999**, *43*, 395-402.
16. G. Chen, S. Liu and S. Chen, *Macromo.l Chem. Phys.*, **2001**, *202*, 1189-1193.
17. G. Chen, S. Liu and S. Zhang, *Macromol. Rapid. Commun.*, **2000**, *21*, 746-749.
18. J. C. Huang, Z. Zhu and J. Yin, *Polymer*, **2001**, *42*, 873-877.
19. A. Tabtiang, S. Lumlong and R. A. Venables, *Europ Polym J.*, **2000**, *36*, 68-81.
20. R. Krishnamoorti and E. P. Giannelis, *Macromolecules*, **1997**, *30*, 4097-4102.
21. H. K. Tae, T. L. Sung and C. H. Lee, *J. Appl. Polym. Sci.*, **2003**, *87*, 2106-2112.
22. B. Hoffmann, J. Kressler and G. Stoppelmann, *Colloid. Polym. Sci.*, **2000**, *278*, 629-636.
23. B. Hoffmann, C. C. Dietrich and R. Thomann, *Macromol Rapid Commun.*, **2000**, *21*, 57-61.
24. M. Alexandre and P. Dubois, *Mater. Sci. Eng. R.*, **2000**, *28*, 1-63.